Applied Microbiology and Biotechnology (2020) 104:10755–10768
https://doi.org/10.1007/s00253-020-10962-9

ENVIRONMENTAL BIOTECHNOLOGY

Octadecyl 3-(3, 5-di-tert-butyl-4-hydroxyphenyl) propanoate, an antifungal metabolite of *Alcaligenes faecalis* strain MT332429 optimized through response surface methodology

Sayed E. El-Sayed[1] · Neveen A. Abdelaziz[1] · Ghadir S. El-Housseiny[2] · Khaled M. Aboshanab[2]

Received: 29 July 2020 / Revised: 6 October 2020 / Accepted: 12 October 2020 / Published online: 22 October 2020
© Springer-Verlag GmbH Germany, part of Springer Nature 2020

Abstract

In the current study, a soil bacterial isolate F2 expressed a significant antagonistic activity against *Candida albicans* ATCC 10231 and *Aspergillus niger* clinical isolate confirmed through cross streak, dual culture, and agar well diffusion methods. The isolate F2 was identified using phenotypic and molecular approaches as *Alcaligenes* (*A.*) *faecalis* MT332429. The identification and structural characterization of the antifungal compound was performed using advanced spectroscopic techniques including UV absorbance, ^{1}H and ^{13}C NMR and 2D NMR (COSY, HSQC, and HMBC) and was identified as octadecyl 3-(3,5-di-tert-butyl-4-hydroxyphenyl) propanoate. Response surface methodology (RSM) using a central composite design was employed to optimize the nutritional and cultural variables affecting the antifungal metabolite yield. The optimum conditions were found to be temperature 30 °C, agitation 150 rpm, glucose 1 g/l, peptone 2 g/l, and pH 8. A confirmatory experiment was performed to assess the accuracy of the optimization procedure, where an increase in the antifungal metabolite production by about 2.48-fold was obtained. To the best of our knowledge, this is the first report of octadecyl 3-(3, 5-di-tert-butyl-4-hydroxyphenyl) propanoate recovered from the culture broth of *A. faecalis* MT332429 with a promising antifungal activity along with its optimized production through RSM.

Key points

- *A novel soil bacterial isolate, F2, identified as Alcaligenes faecalis MT332429, showed significant antagonistic activity against Candida albicans ATCC 10231 and Aspergillus niger clinical isolate.*
- *This stable fungicidal extracellular metabolite was identified as octadecyl 3-(3,5-di-tert-butyl-4-hydroxyphenyl) propanoate.*
- *Optimization using central composite design resulted in 2.48-fold increase in production reaching 213.82 μg/ml.*

Keywords Antifungal · *Alcaligenes faecalis* · Di-tert-butylphenol · Optimization · Spectral analyses · Central composite design

Electronic supplementary material The online version of this article (https://doi.org/10.1007/s00253-020-10962-9) contains supplementary material, which is available to authorized users.

✉ Khaled M. Aboshanab
aboshanab2012@pharma.asu.edu.eg

Sayed E. El-Sayed
sayed.emad@acu.edu.eg

Neveen A. Abdelaziz
neveen.abdelaziz@acu.edu.eg

Ghadir S. El-Housseiny
ghadir.elhossaieny@pharma.asu.edu.eg

[1] Department of Microbiology and Immunology, Faculty of Pharmacy, Ahram Canadian University, POB: 12451, Sixth of October City, Giza, Egypt

[2] Department of Microbiology and Immunology, Faculty of Pharmacy, Ain Shams University, Organization of African Unity St., POB: 11566, Cairo, Abbassia, Egypt

Introduction

Soil microbial communities confer a diverse and complex system (Li and Wu 2018). In an environment supporting the growth of mixed bacterial and fungal flora, complicated interactions are inevitable. Secondary metabolites with antifungal activity grant bacteria an ecological benefit in such environments. This activity has been demonstrated with a range of in vitro methods and provided the basis for the development of many therapeutic antifungal drugs (Coleman et al. 2011).

For instance, purification of the active metabolites from the soil-derived *Streptomyces nodosus* brought about one of the most active antifungal agents, amphotericin B (Donovick et al. 1955). Similarly, nystatin is produced by *Streptomyces noursei* and pyrrolnitrin is produced by *Pseudomonas pyrrocinia* (Kerr 1999). In addition, chemical modifications of these microbial secondary metabolites helped to produce semi-synthetic antifungals with improved activity (Ryley et al. 1981). Scientists endeavors to exploit fungal growth inhibition by bacteria have been fueled by the high morbidity and mortality rates caused by elevated fungal resistance rates (Fuller et al. 2019; Pérez-Cantero et al. 2019; Shishodia et al. 2019). Fungal diseases affect over 1 billion people worldwide, which poses a great risk to immunosuppressed patients and those with underlying chronic illnesses (Buil et al. 2020; Chakrabarti 2020). Consequently, development of new antifungals is crucial, yet the implementation is so far with limited success (Padmavathi et al. 2015). The genus *Alcaligenes* is known among the bacteria having antagonistic activity against various pathogens (Austin 1989). *A. faecalis* inhibits growth of *C. albicans*, and *Alcaligenes sp.* UC9152 inhibits growth of a broad variety of pathogenic fungi (Kerr 1999). Moreover, the symbiotic bacteria *A. faecalis* of the entomopathogenic nematodes *Oscheius* spp. exhibited potential biocontrol of plant and entomopathogenic fungi (Shan et al. 2019). Organic products with branched tert-butyl moieties constitute a variety of bioactive compounds (Bisel et al. 2008; Wang et al. 2017) of which more than 200 are from natural sources (Dembitsky 2006).The 2,4 di tert-butyl phenol moiety has been found in at least 16 species of bacteria in 10 families (Zhao et al. 2020). Other tert-butylphenyl derivatives were obtained from several organisms and demonstrated exceptional antifungal, antibacterial, antioxidant, and antitumor activities (Belghit et al. 2016; Varsha et al. 2015). Constructing the proper nutritional and cultural conditions is very vital for product optimization (Yun et al. 2018). Therefore, this study aimed at the isolation of a promising strain exhibiting antifungal activities and characterization of the purified antifungal metabolite(s), followed by studying various physiological factors influencing the production of the respective metabolite(s) using response surface methodology (RSM). We implemented RSM employing a central composite design (CCD) which reduces the number of trials required to evaluate the interplay between the tested variables (Kavitha et al. 2016; Sun et al. 2010).

Materials and methods

Isolation and phylogenetic analysis of F2 strain

The strain F2 was isolated from a soil sample collected from Gharbia (Tanta, 30.7865° N, 31.0004° E) governorate in Egypt, by agar plate method using trypticase soy agar and incubated at 37 °C for 7 days (Rahman et al. 2011). The strain was identified using microscopical, biochemical, and molecular techniques. We extracted, amplified, and sequenced the DNA coding for 16S ribosomal RNA (16S rRNA) (Moreno-Arribas and Polo 2008).The consensus sequence obtained using the bioedit 7.2 software (https://bioedit.software.informer.com/7.2/) was compared for similarity level with the reference species of bacteria contained in the GenBank database using BLASTn (basic local alignment search tool of nucleotides) (http://blast.ncbi.nlm.nih.gov/Blast.cgi). We used MEGA X (Kumar et al. 2018) for the evolutionary analyses. The 16S rRNA sequence of the F2 strain was aligned using MUSCLE against representative nucleotide sequences retrieved from GenBank. We inferred a phylogenetic tree via likelihood method based on the Tamura-Nei model with a bootstrap analysis (1000 replicates) (Tamura and Nei 1993). The 16S ribosomal RNA sequence was deposited in the NCBI GenBank and in the Culture Collection Ain Shams University (CCASU) belonging to the World Data Centre for Microorganisms (WDCM).

Antifungal activity and indicator microorganisms

Screening of the antifungal activity against *C. albicans* ATCC 10231 was carried out using cross streak assay. The F2 strain was inoculated as a 2-cm wide streak on agar plates and incubated at 37 °C for 24 h to permit metabolite production. Later, *C. albicans* strain was streaked perpendicular to the growth of strain. The plates were inspected after incubation at 28 °C for 48 h to detect the antifungal activity of F2 strain, indicated by the absence of fungal growth (Hossain and Rahman 2014; Peela et al. 2005). The dual culture method was used to detect antifungal activity against *A. niger* clinical isolate (acquired from a patient suffering from chest aspergillosis at Kasr Al-Ainy Hospital, Cairo university, Egypt). Both informed and written consents were obtained after explaining the purpose of the experiment, and the study was approved by the hospital ethics committee and Faculty of Pharmacy ethical committee Nr. ENERC-ASU-230. After initial propagation of *A. niger* on Sabouraud dextrose agar (SDA) medium for 7 days, mycelial fragments (0.5 × 0.5cm) were placed onto another plate on which the F2 strain was cultured simultaneously. Control

plates contained the fungus without the tested isolate (Tiru et al. 2013). After incubation for 7 days at 28 °C, the inhibition zone, which is the distance between the tested isolate and fungal growth, was measured. Moreover, the fungal radial growth inhibition % was calculated (Montealegre et al. 2003), after incubation for 7 days at 28 °C.

$$\text{Inhibition}\ (\%) = \frac{\text{Radial mycelial growth of fungus in (Control−Treatment) plate}}{\text{Radial mycelial growth of fungus in Control plate}} \times 100$$

Additionally, we investigated the fungicidal and/or fungistatic action of the metabolite. A 10-mm culture plug was obtained from the edges of the inhibition zones of the *Alcaligenes* isolate against *Aspergillus niger* and transferred to a fresh SDA plate that was then incubated for 7 days at 28 °C (Navi et al. 2016; Shahidi Bonjar et al. 2005). Growth of *Aspergillus niger* was examined regularly during the incubation period. Absence of growth denoted fungicidal properties while regrowth was suggestive of fungistatic activity of the metabolite produced by *A. faecalis* isolate F2.

Finally, to confirm the antifungal activity, we employed agar well diffusion method (Magaldi et al. 2004). An overnight culture broth of F2 strain was centrifuged at 6000 rpm for 15 min (Centurion Scientific-K240R) to obtain a cell-free supernatant (CFS). Then, the CFS was tested against *C. albicans* ATCC 10231 adjusted spectrophotometrically at 530 nm to obtain a final concentration matching 0.5 McFarland standard. The resulting inhibition zones were measured after incubation of the plates at 28 °C for 24 h. Each experiment was repeated three times, and mean values were recorded (Bundale et al. 2014; Rojas et al. 2006; Wiegand et al. 2008).

Production of the antifungal metabolite

For the production of the antifungal metabolite, a basal medium was prepared according to Singh et al. (2013); it was composed of 5 g/L glucose, 6 g/L Na_2HPO4, 3 g/L K_2HPO4, 1 g/L NH_4Cl, 0.5 g/L NaCl, 0.12 g/L $MgSO_4$, 0.2 g/L $CaCl_2$, and distilled H_2O to 1 L. The pH was adjusted to 7 using KOH pellets before autoclaving. Thirty milliliters of the media were inoculated with strain F2 (3% *v/v*), formerly cultured in trypticase soy broth (TSB) for 15–18 h at 30 °C.

To determine the optimum incubation period, we prepared 7 flasks of the inoculated basal production medium. For 1 week, we sampled one flask per day. The sampled broth was evaluated for antifungal activity using the agar cup plate method (100 μl/well), and we established the optimal incubation time producing expanded inhibition zones.

After the incubation period, 2-ml aliquots were centrifuged for 10 min at 16,000 rpm using a microcentrifuge (Centurion Scientific—K240R), and the supernatant was tested for the presence of extracellular metabolites by cup-plate method on SDA plate. Results were compared to those obtained from sonicating the precipitated cells to release intracellular metabolites, if any (Pinu and Villas-Boas 2017). Each experiment was repeated three times, and mean values of the diameters of inhibition zones were calculated.

Extraction and purification

The fermentation broth was centrifuged, and the CFS was extracted with an equal volume of organic solvent. Eight solvents were used: ethyl acetate (EA), chloroform, hexane, dichloromethane, diethyl ether, *n*-butanol, ethanol, and methanol (Bhosale et al. 2018). Each extract was evaporated using a rotary evaporator (Staurt RE300) at 45 °C (Chawawisit et al. 2015) until dry. Extracts were examined for their antifungal activities using agar well diffusion technique as described above and the respective solvents as negative controls (Bhosale et al. 2018; Kumar et al. 2014). The solvent that resulted in the largest zone of inhibition and highest extraction yield was used for subsequent extraction processes (Parthasarathi et al. 2012). Afterwards, we purified the antifungal metabolite using chromatography silica gel column (3.5 × 80 cm) mesh size 60–120 (Merck, Germany).We used linear gradients of increasing polarity for the solvents chloroform and ethyl acetate and adjusted the flow rate to 1 ml/min (Bhosale et al. 2018).

Fractions were collected at regular intervals, spotted on thin layer chromatography (TLC) plates, and developed with the same solvent system. Elutions with similar retardation factor (R_F) were pooled together. Pooled fractions (PFs) were dried, weighed, and checked for their antifungal activity using the bioautography method against *C. albicans* ATCC 10231 (Chawawisit et al. 2015). Briefly, the TLC plates were placed in petri dishes and overlaid with SDA previously seeded with *C. albicans*. After incubation, clear areas with no growth indicated the location of the active compound (Balouiri et al. 2015). Fractions with the most potent antifungal activity were purified once more by the above column chromatography method, and then purity was checked using TLC plates. Purity was confirmed by visualization of a single spot under UV lamp (UVitec®) at 254 nm and 365 nm.

To correlate between the metabolite concentration and inhibition zone diameter, the fraction with the most potent antifungal activity was purified once more by the previous steps then diluted in DMSO to prepare the following

concentrations: 20.6, 30.8, 40.2, 44.7, 52.5, 60.4, 70.7, 80.3, and 91.1 μg/ml. Two hundred microliters of each concentration were used to test for antifungal activity using the agar well diffusion method as described before (Augustine et al. 2005). After incubation at 28 °C for 24 h, the inhibition zones were measured and plotted against the corresponding concentrations.

We also determined the physical and chemical stability of the antifungal metabolite (data provided in the supplementary file).

Spectral analysis of the antifungal metabolite

One milligram of sample was dissolved in 10-ml DMSO and Shimadzu UV-1800 spectrophotometer was used to record the ultraviolet (UV) spectrum in the range 200–400 nm. One-dimensional (1D) and two-dimensional (2D) NMR spectroscopic data were measured in methanol on Bruker® Avance III HD (400 MHz (^{1}H) and 100 MHz (^{13}C) spectrometer, Germany, equipped with a 5-mm broad-band multinuclear (PABBO) probe. The chemical shifts were reported in parts per million (ppm) relative to TMS (δ0.0) used as internal standard, and the coupling constants (J) were reported in Hertz (Hz). All the ^{1}H and ^{13}C signals were assigned using ^{1}H—^{1}H COSY, ^{1}H—^{13}C HSQC, and ^{1}H—^{13}C HMBC experiments. All spectroscopic measurements were performed at Drug Discovery and Development Research Center at Faculty of Pharmacy, Ain Shams University, Abbassia, Cairo, Egypt.

Factors influencing the production of the antifungal metabolite

Effect of different media components

"One-factor-at-a-time" (OFAT) approach was used for the screening of essential media components for the greatest antifungal production. The original carbon source (glucose) was substituted with one of the following carbon sources (5 g/L): glycerol, starch, lactose, or sucrose. Similarly, the original nitrogen source (ammonium chloride) was replaced with one of the following nitrogen sources (1 g/L): casein, urea, yeast, or peptone, using the optimum selected carbon source. Each experiment was done in triplicate, and the mean values of corresponding inhibition zones were recorded (Singh et al. 2013). Optimum carbon and nitrogen sources were selected for further experiments.

Production optimization using RSM

Face-centered central composite design (CCD) was chosen for the optimization process (Zhang and Zhang 2008). The five factors to be optimized included carbon source (factor A), nitrogen source (factor B), pH (factor C), temperature (factor D), and agitation rate (factor E). Three levels of each factor were tested as shown in Table 1, and a total of 27 runs were carried out as mentioned above, and, one response value, the inhibition zone diameter, was measured accordingly after 4 days of incubation. A second-order polynomial equation, which admits all interaction terms, was derived from the software and used to calculate the predicted responses. The design of experiments was performed using Design Expert® v. 7.0 (Design Expert® Software, Stat-Ease Inc., Statistics Made Easy, Minneapolis, MN, USA). We generated three-dimensional response surface plots to explain the relationships between the 5 experimental variables and the inhibition zone diameters.

Confirmation of the RSM optimization results

The numerical optimization function in the Design Expert® Software was used to obtain the suggested optimal culture conditions, and a new experiment was attempted using these optimal parameters. Antifungal metabolite concentration obtained using these conditions was compared with that obtained using the unoptimized ones.

Statistical analysis

All experiments were carried out in triplicates, and the reported results are the means ± the standard error. Design Expert® v. 7.0 was used for data analysis, response surfaces, and generating the model diagnostic plots. We statistically validated the experimental data by the analysis of variance (ANOVA) indicating the significance of each factor by the reported P values.

Data availability

All data generated or analyzed during this study are included in the published article. New sequences identified in this study have been deposited in NCBI GenBank with the accession number MT332429 (http://www.ncbi.nlm.nih.gov)

Table 1 Factors and levels used in RSM central composite design for optimization of antifungal production

Symbols	Factor	Level		
		−1	0	+1
A	Glucose (g/l)	1	3	5
B	Peptone (g/l)	1	3	5
C	pH	6	7	8
D	Temperature (°C)	30	35	40
E	Agitation rate (rpm)	150	225	300

Results

Identification and phylogenetic analysis of the bacterial isolate F2

Isolate F2 exhibited significant antifungal activity against *C. albicans* in the cross-streak plate method (Fig. 1S) and against *A. niger* in the dual culture method (Fig. 2S). The inhibition zone in the dual culture method against *A. niger* was found to be 10 ± 0.5 mm. In the agar well diffusion method, isolate F2 resulted in an inhibition zone of 15 ± 0.25 mm against *C. albicans*. Isolate F2 proved to exhibit a fungicidal effect and therefore was studied in detail. It was identified as a non-spore-forming Gram-negative bacteria with the following biochemical reactions: negative gelatin liquefaction, urease production, starch, and casein hydrolysis. On the contrary, it was positive for catalase, oxidase, and citrate utilization. The partial 16S rDNA sequence (1335 nucleotides) of strain F2 was determined and deposited in GenBank under the accession number MT332429 and also in the Culture Collection Ain Shams University (CCASU) belonging to the World Data Centre for Microorganisms (WDCM) (strain number, CCASU301 MK212927). Using *A. faecalis* MT332429 as the query sequence for a similarity search via BLASTn revealed 98.8% similarity to NCBI reference sequence of *A. faecalis* subsp. *parafaecalis* strain G (NR_025357.1). The constructed phylogenetic tree also confirmed their close relatedness (Fig. 3S).

Kinetics of the antifungal metabolite(s) production

Optimum antifungal concentration, indicated by an average inhibition zone of 19 mm, was obtained after 4 days of incubation, which was chosen as the ideal incubation time in the following experiments (Fig. 4S).

Extraction and purification of the antifungal metabolite(s)

The antifungal metabolite was extracellularly secreted in the culture broth of *A. faecalis*. Of the tested solvents, ethyl acetate was the best for extraction yielding a maximum dry weight of 0.91 g from 400 ml of culture broth and the largest inhibition zones of 20.6 mm and 19.6 mm against *C. albicans* and *A. niger*, respectively (Table 2).

Chloroform: ethyl acetate was the solvent system utilized in the purification process combining silica gel chromatography and silica thin-layer chromatography (TLC). A total of 140 fractions were eluted and combined into 21 pooled fractions (PFs) based on their TLC profiles (Table 3). Purity was confirmed by visualization of a single spot under UV lamp (UVitec®) at 254 nm and 365 nm (Fig 5S). Elutes 114-118 forming the PF 17 showed the greatest antifungal activity in the bioautography assay and were obtained using chloroform/ethyl acetate with the ratio 20:80 (Table 3).

Table 2 The yield of different solvent extracts obtained from 400 ml of culture broth and the corresponding inhibition zones against *C. albicans* and *A. niger*

Solvent	Yield of extraction (g)	Mean inhibition zones (mm) ± SD	
		C. albicans	*A. niger*
Ethyl acetate	0.91	20.6 ± 0.58	19.6 ± 0.45
Chloroform	0.86	19.3 ± 0.33	18.3 ± 0.58
n-hexane	0.62	16.3 ± 0.25	17.0 ± 0
Dichloromethane	0.58	14.6 ± 0.58	15.3 ± 0.3
Diethyl ether	0.30	12.3 ± 0.67	13 ± 0
n-butanol (*n*-butyl alcohol)	–	–	–
Ethanol	–	–	–
Methanol	–	–	–

SD standard deviation

Plotting different concentrations of the most potent fraction against the respective inhibition zones (mm) unveiled their linear relationship (Fig. 1), represented by the following equation:

$$Y = 0.1151\,X + 9.0592$$

where Y is the inhibition zone diameter (mm), and X is the concentration of the most potent fraction (μg/ml).

Structure elucidation

The compound was attained as a white-yellow amorphous solid powder. The ultraviolet (UV) absorption spectrum recorded a maximum absorption peak (λ max) at 285 nm.

COSY (Fig. 6S (a)) showed correlations between coupled hydrogens in the ^{1}H NMR spectrum, while HSQC (Fig. 6S (b)) allowed to assign carbons with attached protons. Together with HMBC (Fig. 6S(c)) assignments for long-range ^{1}H—^{13}C couplings, connectivity between all groups of the compound was established as listed in Table 4 and Fig. 2.

Thus, the structure of the metabolite was established as octadecyl 3-(3, 5-di-tert-butyl-4-hydroxyphenyl) propanoate. This structure was already reported in the literature; however, this is the first report of its isolation from a culture of *A. faecalis*.

Table 3 Pooled fractions showing ratios of the solvent system used for elution of fractions, the elutes recovered, their retardation factor, dry weight, and inhibition zones against *C. albicans* and *A. niger*

Pooled fractions (PFs)	Ration of chloroform: ethyl acetate	Elutes recovered	Retardation factor (RF)	Dry weight of each PF(g)	Mean inhibition zones (mm) ± SD	
					C. albicans	*A. niger*
1	Chloroform 100%	1–5	0.92	1.4	–	–
2	95:5	6–13	0.11	1.8	–	–
3	90:10	14–21	0.35	4.6	–	–
4	85:15	22–29	0.42	2	–	–
5	80:20	30–45	0.32	3.33	–	–
6	75:25	46–52	0.84	4.1	13.3 ± 0.26	12.6 ± 0.45
7	70:30	53–60	0.53	2.4	17.3 ± 0.33	15.3 ± 0.58
8	65:35	61–66	0.76	4.22	14 ± 1	12.3 ± 0.67
9	60:40	67–70	0.45	2.6	18.3 ± 0.58	16.3 ± 0.25
10	55:45	71–82	0.90	0.99	12.3 ± 0.25	11 ± 1
11	50:50	83–85	0.19	0.89	15.6 ± 0.45	16.3 ± 0.25
12	45:55	86–89	0.27	4	12.6 ± 0.45	11 ± 1
13	40:60	90–95	0.68	3.9	14.3 ± 0.36	13 ± 1
14	35:65	96–100	0.49	3.7	16.6 ± 0.6	14.3 ± 0.33
15	30:70	101–107	0.70	1.67	19.3 ± 0.26	17.6 ± 0.26
16	25:75	108–113	0.88	2.78	20.3 ± 0.33	21 ± 1
17	20:80	114–118	0.67	4.4	22.6 ± 0.2	21.6 ± 0.3
18	15:85	119–126	0.58	1.8	21.6 ± 0.67	19.6 ± 0.45
19	10:90	127–133	0.24	1.01	12 ± 1	13.33 ± 0.2
20	5:95	134–137	0.36	5.2	11.3 ± 0.3	13 ± 1
21	Ethyl acetate 100%	138–140	0.95	4.9	15 ± 1	18 ± 1

SD Standard deviation

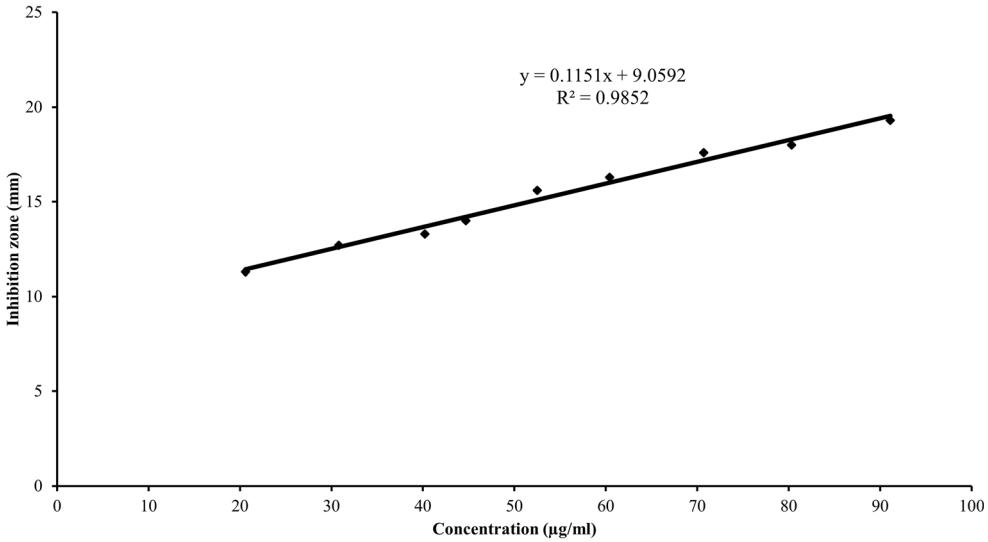

Fig. 1 The linear relationship between the different concentrations of the antifungal metabolite and the inhibition zones

Table 4 ^{1}H NMR and ^{13}C NMR data of the pure metabolite in ppm (multiplicity, *J* in Hz)

Position	δ_H (MeOD, 400 MHz, *J* in Hz)	δ_C (MeOD, 100 MHz)
1	2.85, dd (9.1,6.9)	31.0 (CH_2)
2	2.60, dd (9.1,6.9)	36.5 (CH_2)
3	–	173.4 (C)
1″	4.07, *t*(6.8)	64.6 (CH_2)
2″	1.56–1.61 (m)	29.7 (CH_2)
3″	1.56–1.61 (m)	29.7 (CH_2)
4″-17″	1.24 (m)	22.7–32.0 (CH_2)
18″	0.88, *t*(6.7)	14.1 (CH_3)
1′	–	152.1 (C)
2′	–	135.8 (C)
3′	6.99 (s)	124.8 (CH)
4′	–	131.1 (C)
5′	6.99 (s)	124.8 (CH)
6′	–	135.8 (C)
7′/11′	–	34.3 (C)
(8′–10′)	1.43(s)	30.3 (CH_3)
(12′–14′)	1.43(s)	30.3 (CH_3)
OH	5.07 (bs)	–

Assignments were done based on COSY, HSQC, and HMBC experiments

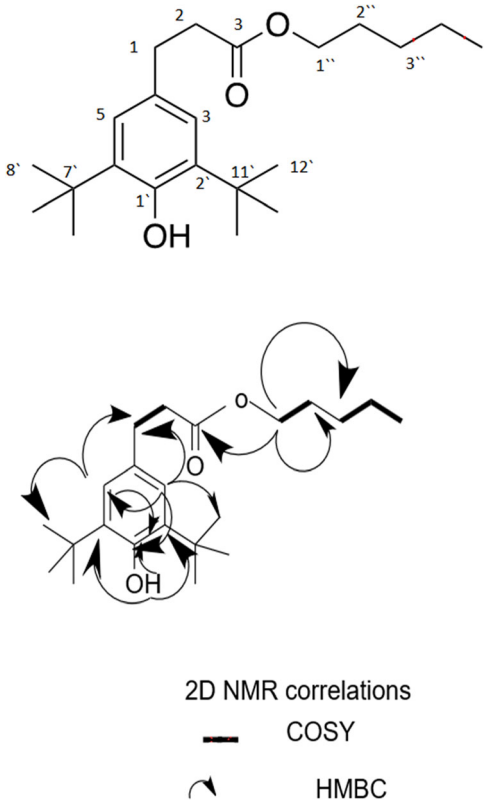

Fig. 2 Chemical structure of the active metabolite produced by *A. faecalis* strain MT332429 based on the spectral data showing ^{1}H NMR, ^{13}C NMR signal assignments and 2D NMR (COSY, HMBC) correlations

Effect of different media components on the metabolite production

Figure 3 depicts the effect of different carbon and nitrogen sources on IZ diameters produced by *A. faecalis* MT332429 against *C. albicans*. Large inhibition zones indicated enhancement in the antifungal metabolite production by *A. faecalis* MT332429. Maximum production was obtained by using glucose (5 g/L) and peptone (1 g/L) as the carbon and nitrogen sources, respectively, and hence, these were selected for further studies.

Optimization of antifungal production using RSM

Table 5 shows the actual values of the tested factors, the design, and the observed results. The relationship between the factors was determined, and a second-order polynomial equation was fitted by the software using the data obtained from the 27 experiments. The resulting RSM model equation obtained from the software is as follows:

$$\begin{aligned} IZ = {} & -423.70218 + 46.12211 \times \text{glucose} + 80.77533 \\ & \times \text{peptone} + 128.97687 \times \text{pH} - 5.04089 \\ & \times \text{temp} - 0.75916 \times \text{agitation} - 3.24967 \times \text{glucose} \\ & \times \text{peptone} - 4.25702 \times \text{glucose} \times \text{pH} - 6.65621 \\ & \times \text{peptone} \times \text{pH} - 0.49030 \times \text{peptone} \\ & \times \text{temp} - 0.039260 \times \text{peptone} \times \text{agitation} \\ & + 0.022993 \times \text{temp} \times \text{agitation} - 1.09545 \times \text{glucose}^2 \\ & + 0.37830 \times \text{peptone}^2 - 6.71680 \times \text{pH}^2 \end{aligned}$$

ANOVA was used to evaluate the significance of the obtained model (Table 6). The F-value of the model was 25.44 (*P* value < 0.0001), which proves the model is significant. The model terms, C, D, E, AB, AC, BC, BD, BE, DE, A^2 and C^2, all having *p* values less than 0.05, are significant model terms. Also, a low coefficient of variation of 7.65 was obtained,

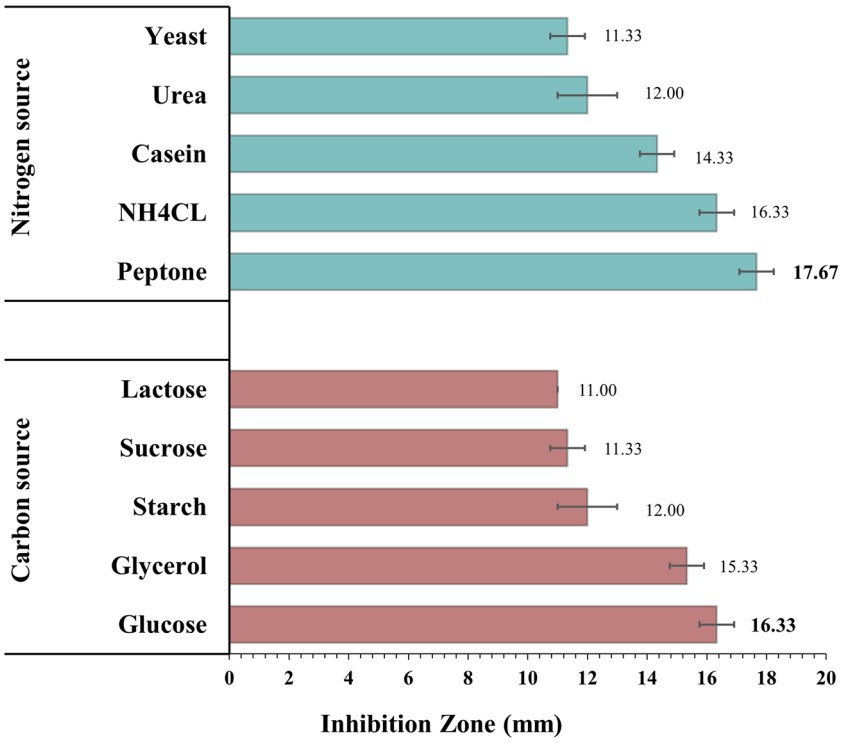

Fig. 3 Effect of different carbon and nitrogen sources on the antifungal activity of *A. faecalis* strain MT332429 against *Candida albicans* ATCC 10231

Table 5 Central composite design runs for the 5 different factors tested showing the observed and predicted responses

Run no.	Glucose (g/l)	Peptone (g/l)	pH	Temperature (°C)	Agitation (rpm)	Observed inhibition zone (mm)	Predicted inhibition zone (mm)
1	3	3	7	35	225	22.6	21.67
2	5	1	8	30	300	24.66	24.31
3	1	5	6	40	300	14.7	14.82
4	1	5	8	30	300	16.6	15.57
5	3	3	8	35	225	15.33	17.16
6	1	1	8	40	300	29.66	29.01
7	1	5	8	40	150	14.66	14.99
8	3	3	7	35	225	22.66	21.67
9	3	3	7	35	225	22.66	21.67
10	1	1	8	30	150	31.8	31.63
11	5	5	6	30	300	11	11.80
12	3	3	6	35	225	14.2	12.75
13	5	5	6	40	150	11.33	11.22
14	3	3	7	35	150	27.66	27.09
15	3	3	7	30	225	25.33	28.37
16	1	3	7	35	225	15.9	17.29
17	3	1	7	35	225	21.33	21.77
18	3	3	7	35	225	22.66	21.67
19	3	3	7	35	300	16.33	16.26
20	3	3	7	35	225	22.66	21.67
21	5	1	6	40	300	23.33	23.98
22	5	3	7	35	225	18.33	17.29
23	3	3	7	40	225	13.33	14.98
24	5	1	8	40	150	19.66	19.79
25	3	5	7	35	225	24.66	24.60
26	5	5	8	30	150	12.5	12.40
27	5	1	6	30	150	26.66	26.61

Table 6 The analysis of variance (ANOVA) of the central composite design (CCD) model for the effects of glucose (A), peptone (B), pH (C), temperature (D), and agitation (E) on the inhibition zones caused by the antifungal metabolite

Source	Sum of squares	Degrees of freedom (df)	Mean square	*F* value	Prob > *F* *P* value
Model	840.87	14	60.06	25.44	< 0.0001
A-Glucose	3.062E−005	1	3.062E−005	1.297E−005	0.9972
B-Peptone	7.84	1	7.84	3.32	0.0934
C-pH	22.48	1	22.48	9.52	0.0094
D-TEMP	196.91	1	196.91	83.40	< 0.0001
E-agitation	128.87	1	128.87	54.58	< 0.0001
AB	221.87	1	221.87	93.97	< 0.0001
AC	216.09	1	216.09	91.52	< 0.0001
BC	232.71	1	232.71	98.56	< 0.0001
BD	85.86	1	85.86	36.37	< 0.0001
BE	123.87	1	123.87	52.46	< 0.0001
DE	235.06	1	235.06	99.56	< 0.0001
A^2	49.67	1	49.67	21.04	0.0006
B^2	5.92	1	5.92	2.51	0.1392
C^2	116.71	1	116.71	49.43	< 0.0001
Residual	28.33	12	2.36		
Corrected total	869.20	26			

denoting the good reliability of the experimental values. The coefficient of determination, R^2, which was 0.97, suggests that 97% of variability in response could be explained by the model. The predicted R^2 (Pred R^2) was 0.8 and was in reasonable agreement with the adjusted R^2 (adj R^2) of 0.93. Finally, the signal to noise ratio, or adequate precision, was equal to 17.82. Consequently, this model was suitable to navigate the design space.

The three-dimensional response surface plots (3D plots) shown in Fig. 4 show how any 2 factors affect our response. By using the numerical optimization function in the Design Expert® software plus these surface plots, the suggested optimum conditions for maximum production of the octadecyl 3-(3, 5-di-tert-butyl-4-hydroxyphenyl) propanoate were found to be glucose 1 g/l, peptone 2 g/l, agitation rate of 150 rpm, a pH of 8, and a temperature of 30 °C.

The following model diagnostic plots were constructed to validate our results:

The normal probability plot of residuals (Fig. 5a) suggests that the residuals follow a normal plot as indicated by the linear pattern.

The Box Cox plot is a useful tool that determines the most appropriate power transformation to be carried out. In this case, the current lambda ($\lambda = 1$) was sufficient (Fig.5b), and no transformation was recommended

The predicted versus actual values plot showed a satisfactory agreement between the projected and the actual data (Fig. 5c).

The residuals versus run number plot showed that the points were arbitrarily distributed around zero (Fig.5d) which implied that the model fits the data.

Confirmatory experiment using optimal conditions

A maximum inhibition zone of 33.67 mm was obtained after carrying out the verification experiment using the suggested optimum condition levels which corresponds to a concentration of 213.82 μg/ml. This value is close to the value predicted by the model which was 36.41 mm. Therefore, the optimal conditions reached brought about a 2.48-fold increase in metabolite concentration as compared with the concentration obtained using the unoptimized conditions (19 mm corresponding to 86.37 μg/ml).

Discussion

The present study investigated the antifungal activity of strain F2 isolated from Egyptian soil. Significant antagonistic activities against human fungal pathogens (*C. albicans* and *A. niger*) were confirmed through cross streak, dual culture, and agar well diffusion methods. Based on its morphological, biochemical properties and 16S rRNA sequence, strain F2 was identified as *A. faecalis*, and its sequence was deposited in NCBI GenBank under the accession number MT332429. This gram-negative isolate was classified in the genus *Alcaligenes*, reported numerously as a source of valuable bioactive agents (Austin 1989). According to Bacic and Yoch (Bacic and Yoch 2001), a marine strain of *A. faecalis* inhibited the growth of clinically important bacteria, especially strains previously shown to be resistant to common antimicrobial agents. In other studies, *A. faecalis* was reported to produce

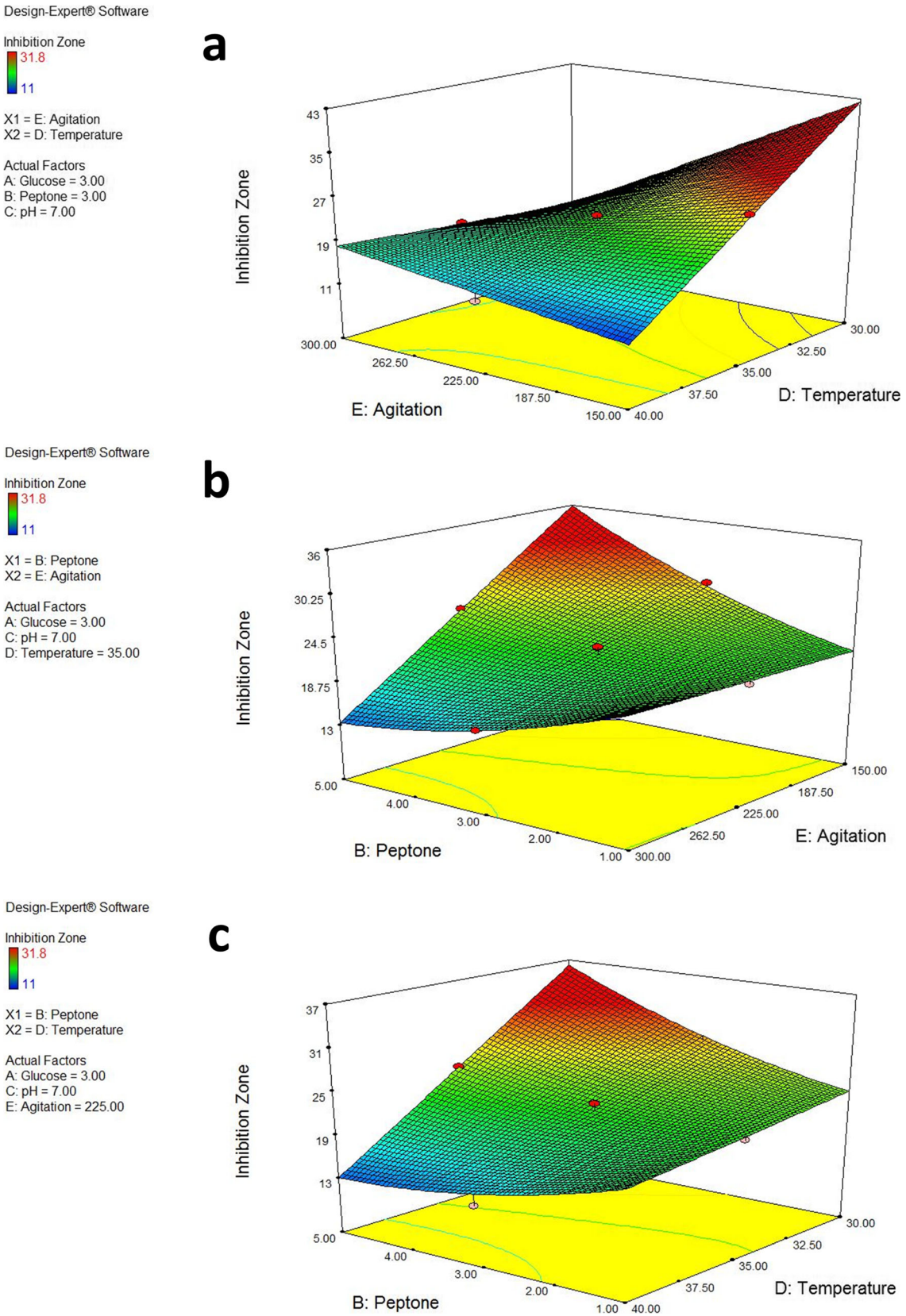

Fig. 4 Three-dimensional response surfaces representing the effect of the five significant parameters on inhibition zone obtained by the metabolite of *A. faecalis strain* MT332429. When the effect of two parameters was plotted, the remaining ones were set at central level **a** agitation and temperature, **b** peptone and agitation, and **c** peptone and temperature.

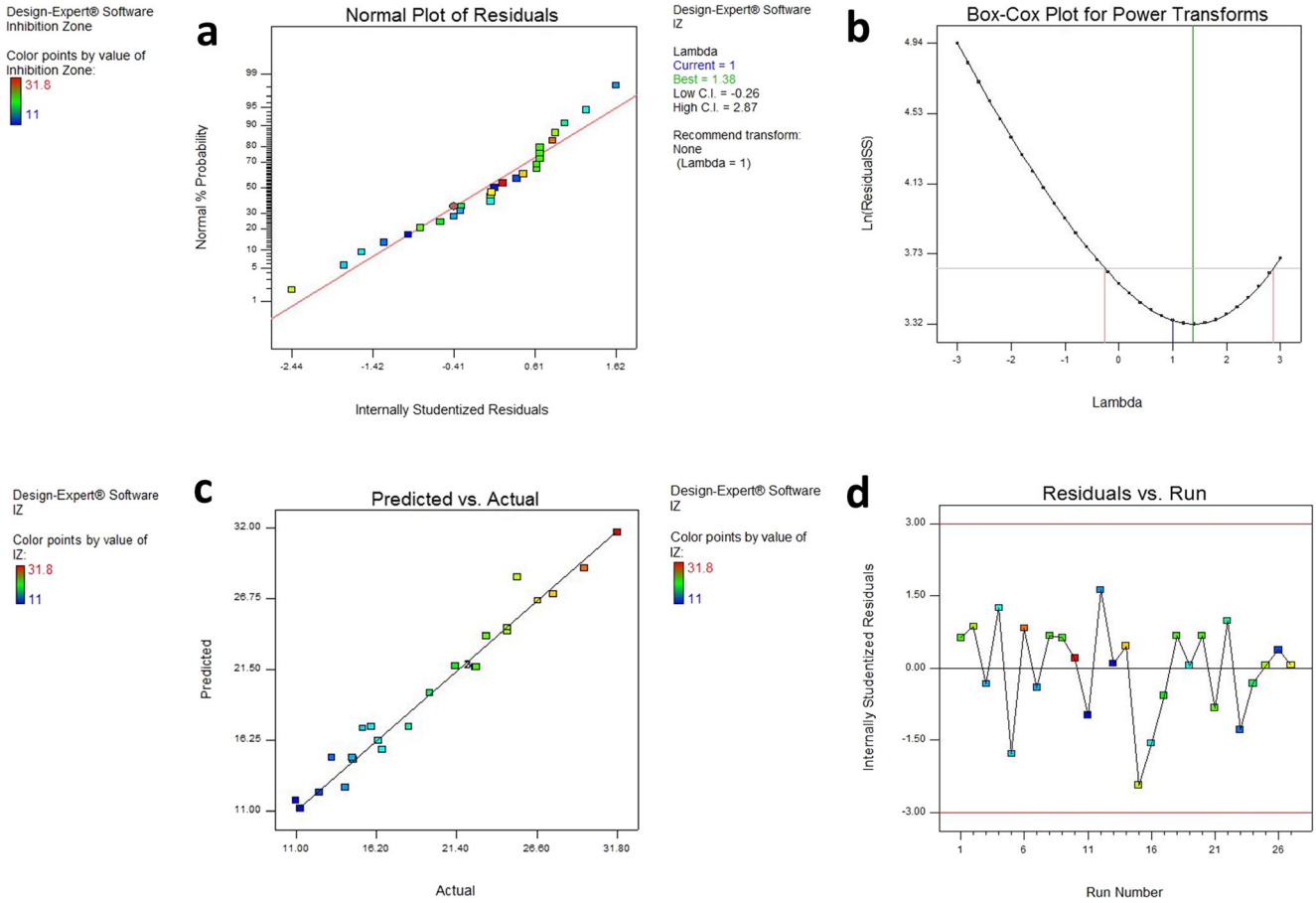

Fig. 5 Model diagnostic plots. **a** The normal probability plot of residuals. **b** Box Cox plot. **c** Predicted versus actual values plot. **d** Residuals versus run number plot

potential antifungal metabolites against certain plant fungal pathogens (Kavroulakis et al. 2010; Moh et al. 2015). Recently, volatiles emitted from *A. faecalis* N1-4 were publicized as an efficient control of several fungal pathogens including aflatoxigenic *Aspergillus flavus* and *Aspergillus niger* (Gong et al. 2019). Furthermore, *A. faecalis* (MRbS12), associated with plants from the Brazilian semi-arid region, produced secondary metabolites with antifungal properties against *C. albicans* CCMB286 (Santoa et al. 2011). In agreement with these reports, our results undoubtedly display the effect of the antifungal metabolite produced by *A. faecalis strain* MT332429 against human pathogenic *C. albicans* and *A. niger*. The metabolite was produced extracellularly and extracted with a maximum yield (0.91 g from 400 ml) using ethyl acetate. One active fraction (PF17) with the highest antifungal activity was identified by silica gel thin layer chromatogram and confirmed by bioautography against *C. albicans*. The metabolite exhibited fungicidal effect which gives it an extra privilege at the pharmacotherapy level.

Based on the 1D and 2D-NMR spectral analyses, we elucidated the molecule is octadecyl 3-(3, 5-di-tert-butyl-4-hydroxyphenyl) propanoate. This compound contains the tert-butyl phenol moiety and can be considered a natural analog to 2,4 di tert-butyl phenol (2,4-DTBP). The 2,4-DTBP was previously reported as a product of many soil bacteria like *Pseudomonas monteilii* and *Streptomyces* spp. It possesses numerous bioactive properties such as antioxidant, antibacterial, and antifungal activities against *C. albicans* and filamentous fungi like *Fusarium* and *Aspergillus* species (Belghit et al. 2016; Padmavathi et al. 2015; Varsha et al. 2015). Additionally, octadecyl 3-(3, 5-di-tert-butyl-4-hydroxyphenyl) propanoate was recently isolated from the culture of *Paenibacillus odorifer* and exhibited mild cytotoxicity against B16 murine melanoma and HaCaT human keratinocyte cell lines (Nguyen et al. 2018), besides its widely characterized antioxidant activity (Neal-Kluever et al. 2015). Even though octadecyl 3-(3, 5-di-tert-butyl-4-hydroxyphenyl) propanoate has been described in literature, this is the first report depicting its antifungal activity and isolation from the soil bacterium *A. faecalis* MT332429. The use of such antioxidant compound as an antifungal agent is a favorable option to avoid hepatotoxic effect of other drugs (Padmavathi et al. 2015).

Microbial production of secondary metabolites is a multifaceted process. Slight changes in the media components and/or conditions can impact the quality and quantity of the

products. We studied the factors affecting the antifungal metabolite production and their interactions to enhance and optimize production. To begin with, the ideal carbon and nitrogen sources were determined using the OFAT approach. Carbon and nitrogen sources are vital ingredients required for bacterial cultivation and metabolite production (Sa-Uth et al. 2018). Carbohydrates are typical carbon source used in bacterial fermentation processes while nitrogen sources may be organic or inorganic (Costa et al. 2002; Sa-Uth et al. 2018). In the present study, glucose and peptone were selected as the optimum media components for maximum metabolite production (Costa et al. 2002).

Next, to optimize the concentrations of the media components and other physiological factors, RSM, an effective statistical approach was employed. RSM has been commonly used for the optimization of antifungal metabolite production by different soil isolates (Souagui et al. 2015). This strategy generates interactive plots and model equations that determine the influence of different parameters on a certain response (Pandian et al. 2014). In contrast to the OFAT approach, this is all achieved with rational resources and time.

The CCD, one of the most popular and efficient designs used, is ideal for successive investigation using a reasonable number of runs (Demirel and Kayan 2012). A total of 27 runs were conducted to study the influence of 5 factors (glucose, peptone, pH, temperature, and agitation) on the metabolite yield. ANOVA, which offers a better understanding about the sources of variation, was used to evaluate the model significance (Mourabet et al. 2017). The large Fisher's value (F-value = 25.44) obtained, which compares between the mean square values of the model and residual error (Kasiri et al. 2013), proved the significance of the model (p value < 0.0001). Generally, for any regression model, an R^2 and adj R^2 value close to 1 reflects high correlation (Chen et al. 2009). Hence, the obtained R^2 value (0.97) indicated the accountability of the model showing an excellent fit of the observed responses with the predicted ones. The obtained adj R^2, which determines whether additional input variables are contributing to the model, was also very good, recorded as 0.93. The ability of the model to precisely predict a response value can be expressed as the pred R^2 which should be in good agreement with the adj R^2; difference between both should not exceed 0.2 (Mourabet et al. 2017). Accordingly, our results displayed a reasonable agreement between the adjusted and pred R^2 values (0.93 and 0.80, respectively). The adequate precision, a ratio of signal to noise, was 17.82, which is greater than 4 and hence implies a satisfactory signal. Moreover, the low CV% of 7.65 suggested the reliability of the experiments (El-Housseiny et al. 2016).

The factors significantly influencing metabolite production were determined by the p value. As shown in the results, the model terms C (pH), D (temperature), E (agitation), A^2, and C^2 were significant ($p < 0.05$), indicating that these are key factors. Moreover, the interactions between the variables AB, AC, BC, BD, BE, and DE were also significant as revealed by the p values attained (< 0.05). For a better understanding of the factors' effects on the antifungal metabolite yield, the model was presented as 3D plots, a three-dimensional representation of the response for selected factors. These plots display the interaction between two variables and allow a direct estimation of the optimal experimental conditions. From these figures and numerical optimization function, the suggested optimum conditions for maximum antifungal metabolite yield were determined and attempted experimentally. A maximum inhibition zone of 33.67 mm was produced by the metabolite which is equivalent to 213.82 μg/ml. Therefore, optimization in our study managed to enhance *A. faecalis* MT332429 production of the antifungal metabolite by about 2.48-fold when compared with that produced by using the unoptimized conditions (86.37 μg/ml). In conclusion, *A. faecalis* isolate MT332429 showed significant antifungal activity against human pathogenic fungi. The active metabolite was extracted, purified, and successfully characterized as octadecyl 3-(3, 5-di-tert-butyl-4-hydroxyphenyl) propanoate. Herein, we report the first isolation of this tert-butyl phenol compound from *A. faecalis* MT332429 soil bacteria. The compound has antifungal activity owing to its tert-butyl phenol moiety which was formerly established to possess antifungal effect. We determined the compound's stability under various physical and chemical conditions. Finally, factors affecting antifungal metabolite production were studied with the help of central composite factorial design in RSM which proved efficiency and accuracy. A maximum concentration of 213.82 μg/ml was reached which corresponds to a 2.48-fold increase in the productivity of our metabolite. This work calls for further studies for large-scale production of this beneficial metabolite scaling up that production.

Acknowledgments We hereby acknowledge the Drug Discovery and Development Research Center at Faculty of Pharmacy, Ain Shams University, Cairo, Egypt, for performing the spectroscopic analysis. We also acknowledge Dr. Ussama Ammar, PhD, student at Korean Institute of Science and Technology; Karim El-Baz, Faculty of Pharmacy, Ain Shams University; and Nada Mosallam, PhD student at Liverpool University for their help in the interpretation of the spectroscopic analyses.

Authors' contributions Conceived and designed the study: KMA, NAA, and GSE. Performed the experiments: SEE. Statistical analysis and figure preparation: NAA, GSE, and SEE;. Drafted the manuscript: NAA ,GSE, and SEE. Wrote the paper in its final format: KMA, GSE, NAA, and SEE. All the authors read and approved the final manuscript.

Compliance with ethical standards

Conflict of interest The authors declare that they have no conflict of interest.

Ethical approval Not applicable

References

Augustine S, Bhavsar S, Kapadnis B (2005) A non-polyene antifungal antibiotic from *Streptomyces albidoflavus* PU 23. J Biosci 30:201–221. https://doi.org/10.1007/bf02703700

Austin B (1989) Novel pharmaceutical compounds from marine bacteria. J Appl bacteriol 67:461–470. https://doi.org/10.1111/j.1365-2672.1989.tb02517.x

Bacic MK, Yoch DC (2001) Antibiotic composition from *Alcaligenes* species and method for making and using the same. Google Patents US6224863B1. https://patents.google.com/patent/US6224863B1/en. Accessed May 2020

Balouiri M, Bouhdid S, Harki E, Sadiki M, Ouedrhiri W, Ibnsouda SK (2015) Antifungal activity of *Bacillus spp*. isolated from Calotropis procera AIT. Rhizosphere against *Candida albicans*. Asian J Pham Clin Res 8:213–217

Belghit S, Driche EH, Bijani C, Zitouni A, Sabaou N, Badji B, Mathieu F (2016) Activity of 2, 4-di-tert-butylphenol produced by a strain of *Streptomyces mutabilis* isolated from a Saharan soil against *Candida albicans* and other pathogenic fungi. J Mycol Med 26:160–169. https://doi.org/10.1016/j.mycmed.2016.03.001

Bhosale H, Kadam T, Mirajgave R, Holkar S (2018) Optimization and characterization of antifungal metabolite from a soil actinomycete *Streptomyces indiaensis* SRT1. Indian J Biotechnol 17:261–271

Bisel P, Al-Momani L, Müller M (2008) The tert-butyl group in chemistry and biology. Org Biomol Chem 6:2655–2665. https://doi.org/10.1039/B800083B

Buil JB, Meijer EF, Denning DW, Verweij PE, Meis JF (2020) Burden of serious fungal infections in the Netherlands. Mycoses 63:625–631. https://doi.org/10.1111/myc.13089

Bundale S, Begde D, Nashikkar N, Kadam T, Upadhyay A (2014) Isolation of aromatic polyketide producing soil *Streptomyces* using combinatorial screening strategies. OALib J 1:1–16. https://doi.org/10.4236/oalib.preprints.1200010

Chakrabarti A (2020) Epidemiology of opportunist fungal infections in Asia Clinical Practice of Medical Mycology in Asia. Springer, pp 51-63

Chawawisit K, Bhoopong P, Phupong W, Lertcanawanichakul M (2015) 2, 4-Di-tert-butylphenol, the bioactive compound produced by *Streptomyces sp*. KB1. J App Pharm Sci 5:007–012. https://doi.org/10.7324/JAPS.2015.510.S2

Chen X-C, Bai J-X, Cao J-M, Li Z-J, Xiong J, Zhang L, Hong Y, Ying H-J (2009) Medium optimization for the production of cyclic adenosine 3′, 5′-monophosphate by *Microbacterium* sp. no. 205 using response surface methodology. Bioresour Technol 100:919–924. https://doi.org/10.1016/j.biortech.2008.07.062

Coleman JJ, Ghosh S, Okoli I, Mylonakis E (2011) Antifungal activity of microbial secondary metabolites. PLoS One 6:e25321. https://doi.org/10.1371/journal.pone.0025321

Costa E, Teixidó N, Usall J, Atarés E, Viñas I (2002) The effect of nitrogen and carbon sources on growth of the biocontrol agent *Pantoea agglomerans* strain CPA-2. Lett Appl Microbiol 35:117–120. https://doi.org/10.1046/j.1472-765X.2002.01133.x

Dembitsky VM (2006) Natural neo acids and neo alkanes: their analogs and derivatives. Lipids 41:309–340. https://doi.org/10.1007/s11745-006-5103-9

Demirel M, Kayan B (2012) Application of response surface methodology and central composite design for the optimization of textile dye degradation by wet air oxidation. Int J Ind Chem 3:24. https://doi.org/10.1186/2228-5547-3-24

Donovick R, Gold W, Pagano J, Stout H (1955) Amphotericins A and B, antifungal antibiotics produced by a *streptomycete. I*. In vitro studies. Antibiot Annu 3:579

El-Housseiny GS, Aboulwafa MM, Aboshanab KA, Hassouna NAH (2016) Optimization of rhamnolipid production by *P. aeruginosa* Isolate P6. J Surfactant Deterg 19:943–955. https://doi.org/10.1007/s11743-016-1845-4

Fuller J, Dingle TC, Bull A, Shokoples S, Laverdière M, Baxter MR, Adam HJ, Karlowsky JA, Zhanel GG (2019) Species distribution and antifungal susceptibility of invasive *Candida* isolates from Canadian hospitals: results of the CANWARD 2011–16 study. J Antimicrob Chemother 74:iv48–iv54. https://doi.org/10.1093/jac/dkz287

Gong A-D, Wu N-N, Kong X-W, Zhang Y-M, Hu M-J, Gong S-J, Dong F-Y, Wang J-H, Zhao Z-Y, Liao Y-C (2019) Inhibitory effect of volatiles emitted from *Alcaligenes faecalis* N1-4 on *Aspergillus flavus* and aflatoxins in storage. Front Microbiol 10. https://doi.org/10.3389/fmicb.2019.01419

Hossain N, Rahman M (2014) Antagonistic activity of antibiotic producing *Streptomyces sp.* against fish and human pathogenic bacteria. Braz Arch Biol Technol 57:233–237. https://doi.org/10.1590/S1516-89132014000200011

Kasiri MB, Modirshahla N, Mansouri H (2013) Decolorization of organic dye solution by ozonation; optimization with response surface methodology. Int J Ind Chem 4:3. https://doi.org/10.1186/2228-5547-4-3

Kavitha G, Kurinjimalar C, Sivakumar K, Kaarthik M, Aravind R, Palani P, Rengasamy R (2016) Optimization of polyhydroxybutyrate production utilizing waste water as nutrient source by *Botryococcus braunii Kütz* using response surface methodology. Int J Biol Macromol 93:534–542. https://doi.org/10.1016/j.ijbiomac.2016.09.019

Kavroulakis N, Ntougias S, Besi MI, Katsou P, Damaskinou A, Ehaliotis C, Zervakis GI, Papadopoulou KK (2010) Antagonistic bacteria of composted agro-industrial residues exhibit antibiosis against soil-borne fungal plant pathogens and protection of tomato plants from *Fusarium oxysporum* f. sp. *radicis-lycopersici*. Plant Soil 333:233–247. https://doi.org/10.1007/s11104-010-0338-x

Kerr JR (1999) Bacterial inhibition of fungal growth and pathogenicity. Microb Ecol Health Dis 11:129–142. https://doi.org/10.1080/089106099435709

Kumar PS, Duraipandiyan V, Ignacimuthu S (2014) Isolation, screening and partial purification of antimicrobial antibiotics from soil *Streptomyces sp*. SCA 7. Kaohsiung J Med Sci 30:435–446. https://doi.org/10.1016/j.kjms.2014.05.006

Kumar S, Stecher G, Li M, Knyaz C, Tamura K (2018) MEGA X: molecular evolutionary genetics analysis across computing platforms. Mol Biol Evol 35:1547–1549. https://doi.org/10.1093/molbev/msy096

Li S, Wu F (2018) Diversity and co-occurrence patterns of soil bacterial and fungal communities in seven intercropping systems. Front Microbiol 9(1521). https://doi.org/10.3389/fmicb.2018.01521

Magaldi S, Mata-Essayag S, Hartung de Capriles C, Perez C, Colella MT, Olaizola C, Ontiveros Y (2004) Well diffusion for antifungal susceptibility testing. Int J Infect Dis 8:39–45. https://doi.org/10.1016/j.ijid.2003.03.002

Moh NMM, Oo KNN, Than WM, Myint M (2015) Study on antifungal activity of *Alcaligenes spp.* by culturing in raw substrates. Int J Tech Res Appl 12:39–43

Montealegre JR, Reyes R, Pérez LM, Herrera R, Silva P, Besoain X (2003) Selection of bioantagonistic bacteria to be used in biological control of *Rhizoctonia solani* in tomato. Electron J Biotechnol 6:115–127. https://doi.org/10.4067/S0717-34582003000200006

Moreno-Arribas MV, Polo MC (2008) Occurrence of lactic acid bacteria and biogenic amines in biologically aged wines. Food Microbiol 25:875–881. https://doi.org/10.1016/j.fm.2008.05.004

Mourabet M, El Rhilassi A, El Boujaady H, Bennani-Ziatni M, Taitai A (2017) Use of response surface methodology for optimization of fluoride adsorption in an aqueous solution by Brushite. Arab J Chem 10:S3292–S3302. https://doi.org/10.1016/j.arabjc.2013.12.028

Navi S, Rajasab A, Yang X (2016) In vitro evaluation of commercial fungicides against some of the major soil borne pathogens of soybean. J Plant Pathol Microbiol 7:340–347. https://doi.org/10.4172/2157-7471.1000340

Neal-Kluever AP, Bailey AB, Hatwell KR (2015) Safety assessment for octadecyl 3-(3, 5-di-tert-butyl-4-hydroxyphenyl)-propionate (CAS Reg. No. 2082-79-3) from use in food contact applications. Food Chem Toxicol 86:176–190. https://doi.org/10.1016/j.fct.2015.10.004

Nguyen T-B-L, Delalande O, Rouaud I, Ferron S, Chaillot L, Pedeux R, Tomasi S (2018) Tert-butylphenolic derivatives from *Paenibacillus odorifer*—A Case of Bioconversion. Molecules 23:1951. https://doi.org/10.3390/molecules23081951

Padmavathi AR, Bakkiyaraj D, Thajuddin N, Pandian SK (2015) Effect of 2, 4-di-tert-butylphenol on growth and biofilm formation by an opportunistic fungus *Candida albicans*. Biofouling 31:565–574. https://doi.org/10.1080/08927014.2015.1077383

Pandian SRK, Deepak V, Sivasubramaniam SD, Nellaiah H, Sundar K (2014) Optimization and purification of anticancer enzyme L-glutaminase from *Alcaligenes faecalis* KLU102. Biologia 69:1644–1651. https://doi.org/10.2478/s11756-014-0486-1

Parthasarathi S, Sathya S, Bupesh G, Manikandan M, Kim C, Manikandan T, Balakrishnan K (2012) Isolation, characterization and extraction of antimicrobial compound from marine actinomycete *Streptomyces hygroscopicus* BDUS 49. Res J Biotechnol 8:3

Peela S, Kurada VB, Terli R (2005) Studies on antagonistic marine actinomycetes from the Bay of Bengal. World J Microbiol Biotechnol 21:583–585. https://doi.org/10.1007/s11274-004-3493-5

Pérez-Cantero A, López-Fernández L, Guarro-Artigas J, Capilla J (2019) Update and recent advances on azole resistance mechanisms in *Aspergillus*. Int J Antimicrob Agents 55:105807. https://doi.org/10.1016/j.ijantimicag.2019.09.011

Pinu FR, Villas-Boas SG (2017) Extracellular microbial metabolomics: the state of the art. Metabolites 7. https://doi.org/10.3390/metabo7030043

Rahman MA, Islam MZ, Islam MA (2011) Antibacterial activities of actinomycete isolates collected from soils of rajshahi, bangladesh. Biotechnol Res Int 2011:857925–857926. https://doi.org/10.4061/2011/857925

Rojas JJ, Ochoa VJ, Ocampo SA, Muñoz JF (2006) Screening for antimicrobial activity of ten medicinal plants used in Colombian folkloric medicine: a possible alternative in the treatment of non-nosocomial infections. BMC Complement Altern Med 6:2. https://doi.org/10.1186/1472-6882-6-2

Ryley JF, Wilson RG, Gravestock MB, Poyser JP (1981) Experimental approaches to antifungal chemotherapy. Adv Pharmacol 18:49–176

Santoa S, Oliveira LKX, de Melo IS, Velozo E, Roque M (2011) Antifungal activity of bacterial strains from the rhizosphere of *Stachytarpheta crassifolia*. Afr J Biotechnol 10:4996–5000. https://doi.org/10.5897/AJB10.2312

Sa-Uth C, Rattanasena P, Chandrapatya A, Bussaman P (2018) Modification of medium composition for enhancing the production of antifungal activity from *Xenorhabdus stockiae* PB09 by using response surface methodology. Int J Microbiol 2018:3965851–3965810. https://doi.org/10.1155/2018/3965851

Shahidi Bonjar G, Rashid Farrokhi P, Aghighi S, Shahidi Bonjar L, Aghelizadeh A (2005) Antifungal characterization of actinomycetes isolated from Kerman, Iran and their future prospects in biological control strategies in greenhouse and field conditions. Plant Pathol J 4:78–84. https://doi.org/10.3923/ppj.2005.78.84

Shan S, Wang W, Song C, Wang M, Sun B, Li Y, Fu Y, Gu X, Ruan W, Rasmann S (2019) The symbiotic bacteria *Alcaligenes faecalis* of the entomopathogenic nematodes *Oscheius* spp. exhibit potential biocontrol of plant-and entomopathogenic fungi. Microb Biotechnol 12:459–471. https://doi.org/10.1111/1751-7915.13365

Shishodia SK, Tiwari S, Shankar J (2019) Resistance mechanism and proteins in *Aspergillus* species against antifungal agents. Mycol 10:151–165. https://doi.org/10.1080/21501203.2019.1574927

Singh RK, Kumar DP, Solanki MK, Singh P, Srivastva AK, Kumar S, Kashyap PL, Saxena AK, Singhal PK, Arora DK (2013) Optimization of media components for chitinase production by chickpea rhizosphere associated *Lysinibacillus fusiformis* B-CM18. J Basic Microbiol 5:451–460. https://doi.org/10.1002/jobm.201100590

Souagui Y, Tritsch D, Grosdemange-Billiard C, Kecha M (2015) Optimization of antifungal production by an alkaliphilic and halotolerant actinomycete, *Streptomyces* sp. SY-BS5, using response surface methodology. J Med Mycol 25:108–115. https://doi.org/10.1016/j.mycmed.2014.12.004

Sun Y, Liu J, Kennedy JF (2010) Application of response surface methodology for optimization of polysaccharides production parameters from the roots of *Codonopsis pilosula* by a central composite design. Carbohydr Polym 80:949–953. https://doi.org/10.1016/j.carbpol.2010.01.011

Tamura K, Nei M (1993) Estimation of the number of nucleotide substitutions in the control region of mitochondrial DNA in humans and chimpanzees. Mol Biol Evol 10:512–526. https://doi.org/10.1093/oxfordjournals.molbev.a040023

Tiru M, Muleta D, Bercha G, Adugna G (2013) Antagonistic effect of rhizobacteria against coffee wilt disease caused by *Gibberella xylarioides*. Asian J Plant Pathol 7:109–122. https://doi.org/10.3923/ajppaj.2013.109.122

Varsha KK, Devendra L, Shilpa G, Priya S, Pandey A, Nampoothiri KM (2015) 2, 4-Di-tert-butyl phenol as the antifungal, antioxidant bioactive purified from a newly isolated *Lactococcus sp*. Int J Food Microbiol 211:44–50. https://doi.org/10.1016/j.ijfoodmicro.2015.06.025

Wang Y, Schnell B, Baumann S, Müller R, Begley TP (2017) Biosynthesis of branched alkoxy groups: iterative methyl group alkylation by a cobalamin-dependent radical SAM enzyme. J Am Chem Soc 139:1742–1745. https://doi.org/10.1021/jacs.6b10901

Wiegand I, Hilpert K, Hancock RE (2008) Agar and broth dilution methods to determine the minimal inhibitory concentration (MIC) of antimicrobial substances. Nat Protoc 3:163–175. https://doi.org/10.1038/nprot.2007.521

Yun TY, Feng RJ, Zhou DB, Pan YY, Chen YF, Wang F, Yin LY, Zhang YD, Xie JH (2018) Optimization of fermentation conditions through response surface methodology for enhanced antibacterial metabolite production by *Streptomyces sp*. 1-14 from cassava rhizosphere. PLoS One 13:e0206497. https://doi.org/10.1371/journal.pone.0206497

Zhang Y, Zhang J (2008) Optimization of headspace solid-phase microextraction for analysis of ethyl carbamate in alcoholic beverages using a face-centered cube central composite design. Anal Chim Acta 627:212–218. https://doi.org/10.1016/j.aca.2008.08.014

Zhao F, Wang P, Lucardi RD, Su Z, Li S (2020) Natural sources and bioactivities of 2, 4-di-tert-butylphenol and its analogs. Toxins 12:35. https://doi.org/10.3390/toxins12010035

Publisher's note Springer Nature remains neutral with regard to jurisdictional claims in published maps and institutional affiliations.